

# Non-catalytic Behavior of SiO<sub>2</sub> Fine Powders in Presence of Strong Shock Waves for Aerospace Applications

Vishakantaiah Jayaram<sup>1,\*</sup>, Ravichandran Ranjith<sup>2</sup>, Parthasarathi Bera<sup>3</sup>

<sup>1</sup>Solid State and Structural Chemistry Unit, Indian Institute of Science, Bengaluru, India

<sup>2</sup>Department of Aerospace Engineering, Indian Institute of Science, Bengaluru, India

<sup>3</sup>Surface Engineering Division, Council of Scientific and Industrial Research–National Aerospace Laboratories, Bengaluru, India

## Email address

jayaram@iisc.ac.in (V. Jayaram)

\*Corresponding author

## Citation

Vishakantaiah Jayaram, Ravichandran Ranjith, Parthasarathi Bera. Non-catalytic Behavior of SiO<sub>2</sub> Fine Powders in Presence of Strong Shock Waves for Aerospace Applications. *Journal of Materials Sciences and Applications*. Vol. 4, No. 3, 2018, pp. 37-46.

**Received:** February 16, 2018; **Accepted:** March 21, 2018; **Published:** May 16, 2018

---

**Abstract:** Application of shock tubes for the interaction of shock-heated test gases with SiO<sub>2</sub> fine powders has been demonstrated for the first time in this work. Fine SiO<sub>2</sub> powders are made to interact with shock-heated test gases at reflected shock temperatures of 1960–3990 K (estimated) inside the shock tube for millisecond (ms) time scale. The objective of the work is to investigate the behavior of SiO<sub>2</sub> powders upon interaction with the high temperature shock-heated nitrogen gas. The SiO<sub>2</sub> samples are characterized using different experimental techniques to understand the effects of shock interaction and to study the non-catalytic behavior of SiO<sub>2</sub> powders as it form new compounds on interaction with test gases at the experimentally simulated high temperature conditions. The high temperature imparted by shock wave is absorbed by SiO<sub>2</sub> and undergoes phase transformation as evident from the XRD patterns. SEM and TEM studies show the formation of spherical particles after shock treatment due to the superheating and cooling of fine powders. XPS studies show the formation of silicon nitride and silicon oxy-nitride resulting from the interaction of high temperature nitrogen gas, confirming the non-catalytic behavior of SiO<sub>2</sub> powders.

**Keywords:** Strong Shock Waves, Shock-Powder Interaction, SiO<sub>2</sub> Powders, Non-catalytic Reaction, Nitridation, Millisecond Reaction

---

## 1. Introduction

During atmospheric re-entry, shock wave engulfs the vehicle and gives rise to a strong thermo-chemical non-equilibrium situation inside the shock layer. The gas trapped between the shock layer and the vehicle becomes excited in its degrees of freedom such as vibration and electronic excitation, dissociation and ionization in some cases depending on the temperature of the shock layer [1]. When the dissociated species recombine, they give up the dissociation energy which is transferred as heat flux to the vehicle surface [2, 3]. In addition to that molecular gas at high temperatures might also transfer heat to the vehicle body. The chemical reaction can be both homogeneous and heterogeneous depending on the carrier of the released

energy. The scenario in which the vehicle surface acts as the third body and takes away the energy released from recombination is termed as heterogeneous catalytic surface recombination [4]. The recombination of these atomic species is very critical in estimating the heat flux to the surface, which in turn is significant in designing the thermal protection system (TPS) of a mission [5]. Since the weight reduction in TPS leads to an increase in payload of the mission, understanding the surface reaction mechanisms is critical in the design of an optimized TPS [6]. Many studies have been carried out using plasma arc jet wind tunnels to study the chemical reactions involved during re-entry. The arc discharge facilities introduce metallic contamination from the electrode and hence the catalyticity of the material cannot be estimated properly [7]. Also the plasma arc jet facilities

simulate blunt body stagnation heat transfer [8] but cannot simulate the pressure, density and enthalpy conditions in the flight conditions simultaneously [9]. Moreover, considering the specific test gases such as Ar, N<sub>2</sub> or O<sub>2</sub> will give more insight into the surface reaction mechanisms.

In case of ablative TPS, the material erodes away from the surface and the ablated material might diffuse into the shock layer and forms new product by reacting with the shock-heated gases. This work is aimed at understanding the reaction mechanisms which might occur when the TPS material ablates and interacts with the non-equilibrium gas present during atmospheric re-entry. To understand the reaction mechanisms involved in this interaction of gas species with the TPS material during re-entry, ground test facilities have been established. One such facility is shock tube which can be employed to expose the materials, in the form of thin films, pellets and fine powders, to shock waves [10-12]. The dissociated gas species in shock layer diffuse into the boundary layer and react with the TPS material on the vehicle surface producing new compound(s) out of it. In this context, the present work is taken up by exposing the SiO<sub>2</sub> fine powders to shock waves in presence test gases. SiO<sub>2</sub> is chosen for this study since it has low catalycity and it is used as the base material for most of the TPS, both ablative and reusable [3, 13]. The dependence of catalycity on temperature and pressure is difficult to explain theoretically. The dependence seems to be affected by material type as well as experimental conditions such as temperature range, pressure range and kind of fraction of gas species [7]. Nitridation is done by various other chemical methods such as carbothermal reduction nitridation (CRN) [14], plasma nitridation [15] and diffusion reaction [16], etc. This paper presents a novel method of nitridation by shock waves due to interaction that happens in millisecond timescale. Other than thermal protection, SiO<sub>2</sub> microcapsules can potentially be used in aerospace applications to induce self-healing of the spacecraft coatings [17]. SiO<sub>2</sub> coatings can act as a sealant for cracks and also helps in preventing the external diffusion of carbon by forming a glassy protective layer [18].

The process of shock-induced non-catalytic surface reactions in SiO<sub>2</sub> fine powders is demonstrated in this work by using nitrogen as the test gas in shock tubes. The fundamental reaction mechanisms are studied for a given temperature and pressure condition that would throw some light to make some correlations of catalycity with the given conditions. The

investigation carried out here brings out the non-catalytic behavior of the SiO<sub>2</sub> fine powders upon interaction with shock-heated test gases at given reflected shock pressure and temperature conditions. Different experimental characterization techniques are employed to study the changes in SiO<sub>2</sub> powders before and after shock treatment.

## 2. Experimental Details

### 2.1. Shock Treatment Experiment

The shock-materials interaction experiments were carried out in Material Shock Tube (MST1) indigenously fabricated and installed at Shock Induced Material Chemistry Laboratory, Solid State and Structural Chemistry Unit, Indian Institute of Science, Bengaluru, India. MST1 is comprised of driver and driven section of 2 m and 5 m length respectively with an inner diameter of 80 mm, the schematic diagram of MST1 is shown in Figure 1. The shock tube is operated by conventional method of bursting an Al metal diaphragm of required thickness to produce shock waves of desired strength. The diaphragm used here is made of aluminum, which is placed between the driver and driven section. The driven section is purged with ultra high pure (UHP) Argon (99.999%) for three times and is filled with the required UHP test gas mixture; argon and nitrogen at an equal partial pressure of 0.05 bar each, amounting to 0.1 bar test gas fill pressure. Before filling the test gas mixture, the shock tube is pumped to a high vacuum upto  $\sim 8 \times 10^{-5}$  bar to avoid any gas impurities. The driver section is filled with high pressure helium to burst the diaphragm to produce shock waves. The primary shock wave (at pressure  $P_2$ ) travels inside the driven section and produces reflected shock wave (at pressure  $P_3$ ) as it gets reflected at the end flange of the driven section. To obtain different reflected shock temperatures ( $T_3$ ), Al diaphragms of different thicknesses (3 mm, 2.5 mm, 2 mm and 1.5 mm) are used. Pressure transducers (PCB Piezotronics Model No. 113B22) are mounted at various locations to acquire pressure signals and are recorded by a Tektronix digital oscilloscope (Model no. TBS2014B). The time taken by the shock wave ( $\Delta t$ ) to cross the two given sensor location at known distance ( $\Delta x$ ) is used to find out the shock speed ( $V_s$ ). The shock Mach number ( $M_s$ ) thus calculated is used to calculate the reflected shock temperature ( $T_3$ ) using 1-D normal shock relations [19]:

$$V_s = \frac{\Delta x}{\Delta t}; M_s = \frac{V_s}{a} = \frac{V_s}{\sqrt{\gamma R T_1}} \quad (1)$$

$$\frac{T_3}{T_1} = \frac{\{2(\gamma - 1)M_s^2 + (3 - \gamma)\} \{(3\gamma - 1)M_s^2 - 2(\gamma - 1)\}}{(\gamma + 1)^2 M_s^2} \quad (2)$$

where  $a$  is the speed of sound in test gas mixture,  $\gamma$  is the specific heat ratio of test gas mixture,  $R$  is the gas constant and  $T_1$  is the temperature of test gas mixture. The Al diaphragms of different thicknesses give shock waves at different Mach

numbers ( $M_s$ ) ranging from 3.1 to 4.5 corresponding to different reflected shock temperatures ( $T_3$ ) ranging from 1960 K to 3990 K (estimated) for milliseconds timescale. The values of Mach number, reflected shock pressure and temperature for

all the cases are listed in Table 1. At these shock temperatures, SiO<sub>2</sub> fine powders mounted after the gate valve are exposed to shock waves to study the reaction mechanisms. To understand the effect of number of shock interaction on SiO<sub>2</sub> powders, the fresh samples are exposed to shock wave once (termed as 1-

shock treatment) and twice (termed as 2-shock treatment) at different reflected shock temperatures. Shock heated N<sub>2</sub> gas reacts with SiO<sub>2</sub> in the SiO<sub>2</sub> reaction chamber. Solid residue left after shock tube experiments were collected from the chamber for further analysis.

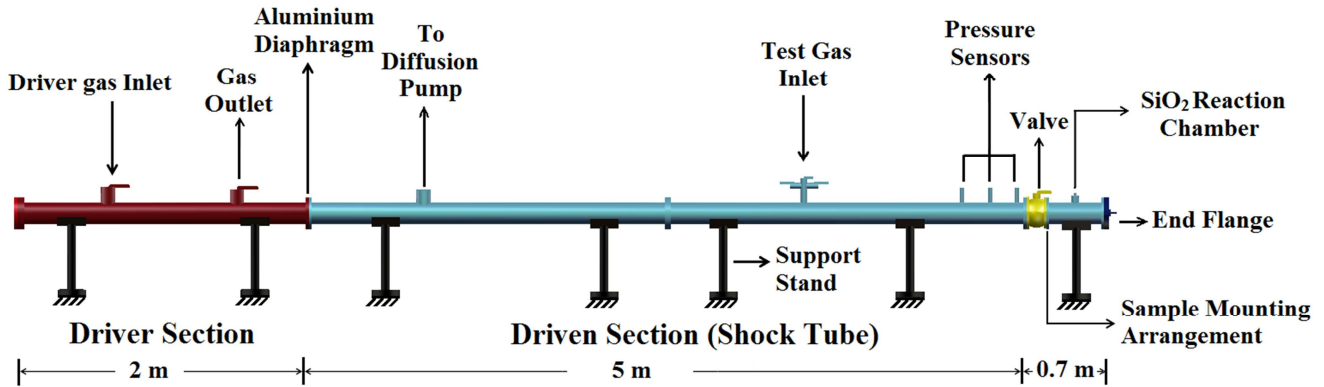


Figure 1. Schematic diagram of material shock tube (MSTI).

Table 1. Shock parameters for different experiments.

Sl. No	Shock Mach number $M_5$	Reflected shock pressure $P_5$ (bar)	Reflected shock temperature $T_5$ (K)
1-shock treatment			
1	4.4	13.2	3790
2	4.2	12.1	3410
3	4.0	10.7	3140
4	3.1	7.3	1960
2-shock treatment			
5	4.5	14.1	3990
6	4.1	10.5	3340
7	4.0	9.9	3250
8	3.3	9.4	2250

## 2.2. Characterization

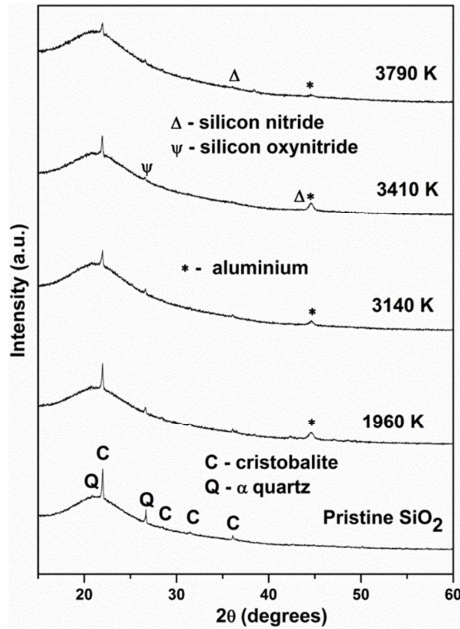
X-ray diffraction (XRD) patterns were obtained for the samples before and after shock treatments to analyze the changes in crystal structure. The XRD patterns were recorded for all the samples at a scan rate of  $2^\circ \text{ min}^{-1}$  with a step size of  $0.013^\circ$  for  $2\theta$  from  $15$  to  $60^\circ$  (PANalytical Empyrean, Cu  $K\alpha$  ( $\lambda$ ) =  $1.5418 \text{ \AA}$ ). Scanning electron microscope (SEM) micrographs were obtained to study the surface morphology of the samples before and after shock treatment (FEI Quanta SIRION) at a working distance of  $5 \text{ mm}$  operating at  $10 \text{ kV}$  accelerating voltage. High resolution transmission electron microscopy (HRTEM) was done using TEM T20 to understand the crystalline nature of the samples before and after shock treatments. X-ray photoelectron spectroscopy (XPS) was done with (AXIS Ultra DLD, Kratos Analytical) using Al  $K\alpha$  ( $1486.6 \text{ eV}$ ) radiation as an X-ray source operated at  $150 \text{ W}$  ( $12 \text{ kV}$  and  $12.5 \text{ mA}$ ) to characterize the electronic structure and chemical composition of the samples. The binding energies reported here were calculated with reference to C1s peak at  $284.5 \text{ eV}$ . All the spectra were obtained with pass energy of  $40 \text{ eV}$  and step increment of  $0.05 \text{ eV}$ . Low energy electron flood gun was used to nullify the charge accumulating on the insulating samples.

## 3. Results and Discussion

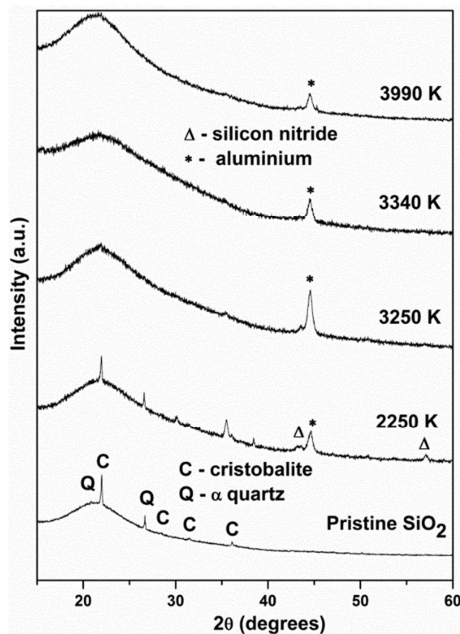
### 3.1. XRD Studies

Fresh SiO<sub>2</sub> sample shows XRD peaks corresponding to the cristobalite (JCPDS No. 01-077-1316) and  $\alpha$ -quartz (JCPDS No. 01-078-1253) phases which are identified from the database and assigned as 'C' and 'Q' respectively as shown in Figure 2. The cristobalite is tetragonal with lattice parameters of  $a = b = 4.971 \text{ \AA}$ ,  $c = 6.928 \text{ \AA}$  and  $\alpha$ -quartz is hexagonal with lattice parameters of  $a = b = 4.912 \text{ \AA}$ ,  $c = 5.402 \text{ \AA}$ . The pristine sample exhibits both crystalline and amorphous nature with two prominent crystalline peaks at  $21.9^\circ$  and  $26.7^\circ$ . Due to interaction with shock in presence of Ar+N<sub>2</sub> test gas mixture, the samples undergo phase transformation from crystalline to amorphous nature with the increasing shock temperature. In addition to this, after 1-shock treatment with Ar+N<sub>2</sub> mixture, SiO<sub>2</sub> forms new compounds such as silicon oxynitride and silicon nitride with traces of unreacted cristobalite and  $\alpha$ -quartz due to shock induced nitridation. The peaks due to silicon nitride and silicon oxynitride are denoted by ' $\Delta$ ' and ' $\psi$ ' respectively as highlighted in Figure 2a. The peak at  $44.5^\circ$  is due to the aluminum impurity from the diaphragm used to produce shock waves, which is indicated by '\*' in Figure 2. After 2-shock treatment, the pristine sample gets completely

converted to amorphous nature indicated by the disappearance of the crystalline peak at  $2\theta = 21.9^\circ$ . Unlike 1-shock treatment, the transformation to amorphous is more pronounced with no traces of crystallinity in the XRD pattern of 2-shock-treated sample. Also the crystal structure of SiO<sub>2</sub> changes from tetragonal to cubic form. Formation of silicon nitride is seen at 2250 K and in the other cases, the crystalline SiO<sub>2</sub> transforms to amorphous nature of oxide or nitride.



(a)



(b)

Figure 2. XRD patterns of SiO<sub>2</sub> powders before and after shock treatment at different temperatures: (a) 1-shock treatment and (b) 2-shock treatment.

3.2. SEM Studies

SEM micrographs of SiO<sub>2</sub> sample before shock treatment

shows irregular shaped particles of different sizes as it can be seen from Figure 3a. After 1-shock treatment at different temperatures, the irregular particles change to spherical particles of different sizes and sponge structures due to reaction with shock heated Ar+N<sub>2</sub> mixture. However, at shock temperature of 1960 K, there is no significant change observed in the surface morphology of SiO<sub>2</sub> powders as shown in Figure 3b. For 1-shock treatment at shock temperature of 3790 K, spherical particles are observed with few unreacted SiO<sub>2</sub> as seen in Figure 3c. When the sample is exposed to 2-shock treatment at the minimum temperature condition (2250 K), few spherical particles are seen due to the interaction of shock twice with the sample as shown in Figure 3d. Due to 2-shock treatment at the maximum temperature (3390 K), the formation of spherical and sponge-type particles are observed as shown in Figure 3e. There are no traces of unreacted SiO<sub>2</sub> after 2-shock treatment. At higher magnifications, even smaller spheres are found to be distributed on the bigger spheres. In some cases, two or more spheres are seen fused together indicating the effect of super heating and cooling due to shock waves.

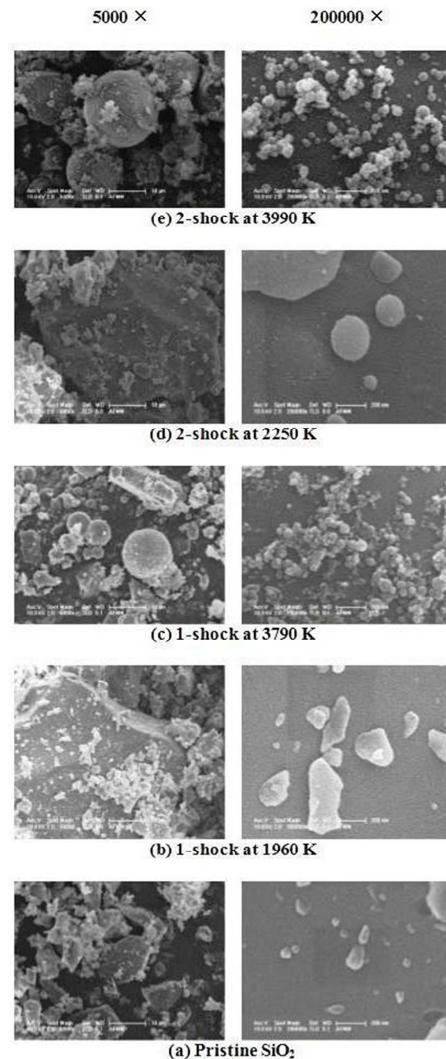


Figure 3. SEM images of SiO<sub>2</sub> powders before and after shock treatment at different temperatures.

### 3.3. TEM Studies

The bright field image of pure  $\text{SiO}_2$  shows irregular particle size as can be seen from Figure 4a. The irregular particles become uniformly spherical after shock treatment. The bright field images of  $\text{SiO}_2$  after one and two shock treatments show uniform spherical particles as can be seen from Figures 4b-4e. The size of the fresh  $\text{SiO}_2$  particles range from 100–500 nm and upon shock interaction they form uniform spheres of varying sizes ranging from 10–300 nm. High resolution TEM images of fresh  $\text{SiO}_2$  exhibits crystalline fringes whereas the shock treated samples are of amorphous nature.

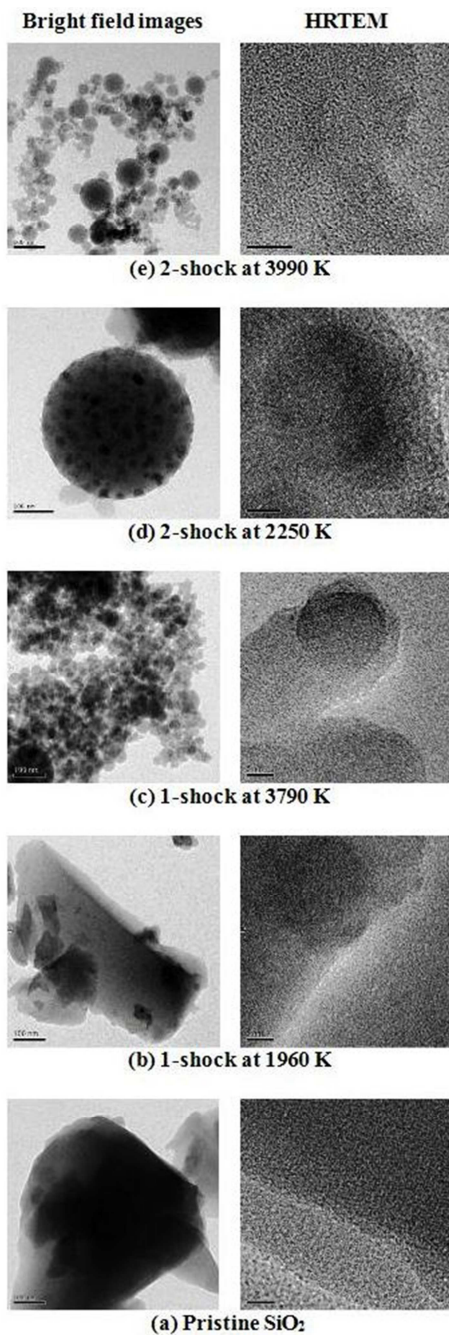
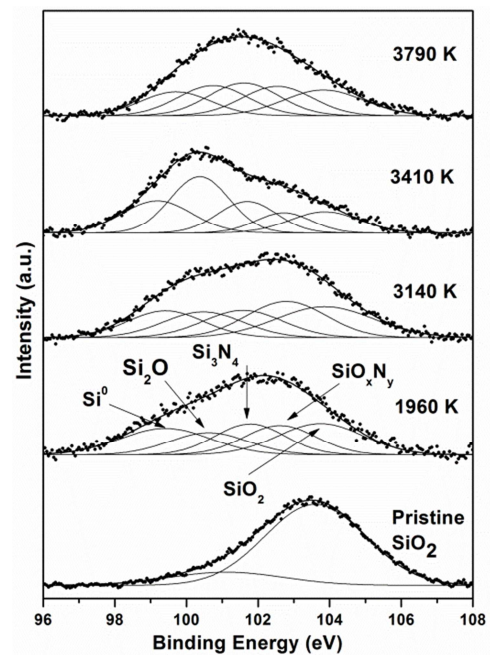


Figure 4. HRTEM images of  $\text{SiO}_2$  powders before and after shock treatment at different temperatures.

### 3.4. XPS Studies

Deconvoluted  $\text{Si}2p$  core levels of the  $\text{SiO}_2$  fine powders and shock-treated samples are shown in Figure 5.  $\text{Si}2p$  binding energy peak positions of different Si species of  $\text{SiO}_2$  samples with different shock-treated conditions are summarized in Table 2. XPS of  $\text{SiO}_2$  powders before shock treatments show peaks due to  $\text{Si-O}$  and  $\text{SiO}_2$  at 101.1 and 103.6 eV respectively. The peak positions are in good agreement with those reported in literature [20]. After the shock treatment of  $\text{SiO}_2$  with  $\text{Ar}+\text{N}_2$  mixture, the  $\text{SiO}_2$  fine powders form new compounds such as silicon nitride and silicon oxynitride, in addition to formation of  $\text{Si}_2\text{O}$  and elemental Si. After 1-shock treatment,  $\text{SiO}_2$  fine powders show formation of new compounds by indicating new peaks corresponding to  $\text{Si}_3\text{N}_4$  and  $\text{SiO}_x\text{N}_y$ . The peak positions of  $\text{Si}_3\text{N}_4$  vary from 101.6–101.8 eV and for  $\text{SiO}_x\text{N}_y$  the peaks vary from 102.5–102.8 eV. The formation of elemental Si is also observed from the presence of peaks in the range of 99.2–99.7 eV in all the shock-treated samples. As the sample would not have been completely reacted and formed into nitride/oxynitride species, some unreacted  $\text{SiO}_2$  is also seen in the shock-treated samples in the range of 103.7–103.8 eV. The peak positions of species for different shock treatment cases are similar to those reported in the literature [21, 22]. The slight variations in the peak position might be an indication of the formation of sub-stoichiometric nitride compounds [22] and mixed phase due to high temperature shock wave interaction with  $\text{SiO}_2$  powders. After 2-shock treatment, similar  $\text{Si}2p$  peaks are observed corresponding to new nitrides in the binding energy range of 101.6–101.9 eV and oxynitrides in the range of 102.6–102.9 eV as shown in Figure 5. Elemental Si is observed in the binding energy range of 99.1–99.5 eV. Peaks corresponding to  $\text{SiO}_2$  are seen in the range of 103.7–104.0 eV.



(a)

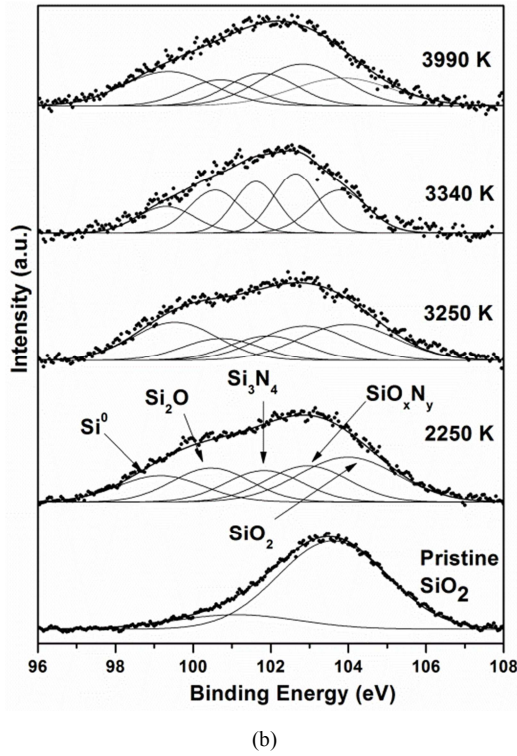


Figure 5. XPS of Si2p core levels of SiO<sub>2</sub> powders before and after shock treatment at different temperatures:(a) 1-shock treatment and (b) 2-shock treatment.

Table 2. Si2p binding energy (eV) positions for different Si based compounds produced after shock-treatment of SiO<sub>2</sub> powders.

T <sub>5</sub>	Si	Si <sub>2</sub> O	SiO	Si <sub>3</sub> N <sub>4</sub>	SiO <sub>x</sub> N <sub>y</sub>	SiO <sub>2</sub>
<b>1-shock treatment</b>						
3790 K	99.7	100.7		101.6	102.5	103.8
3410 K	99.2	100.3		101.7	102.7	103.8
3140 K	99.4	100.4		101.6	102.8	103.8
1960 K	99.4	100.6		101.8	102.6	103.7
Pristine SiO <sub>2</sub>			101.1			103.6
<b>2-shock treatment</b>						
3990 K	99.3	100.7		101.8	102.8	103.8
3340 K	99.3	100.5		101.6	102.6	103.7
3250 K	99.5	100.7		101.9	102.8	104.0
2250 K	99.1	100.4		101.8	102.9	104.0
Pristine SiO <sub>2</sub>			101.1			103.6

Table 3. O1s binding energy (eV) positions for different Si based compounds produced after shock-treatment of SiO<sub>2</sub> powders.

T <sub>5</sub>	SiO	SiO <sub>x</sub> N <sub>y</sub>	SiO <sub>2</sub>
<b>1-shock treatment</b>			
3790 K		531.2	533.3
3410 K	530.9	532.2	533.5
3140 K		531.7	533.7
1960 K		531.4	533.7
Pristine SiO <sub>2</sub>			533.2
<b>2-shock treatment</b>			
3990 K		531.3	533.6
3340 K		531.4	533.5
3250 K	530.8	532.0	533.5
2250 K		532.0	533.5
Pristine SiO <sub>2</sub>			533.2

Table 4. N1s binding energy (eV) positions for different Si based compounds produced aftershock-treatment of SiO<sub>2</sub> powders.

T <sub>5</sub>	Si <sub>3</sub> N <sub>4</sub>	SiO <sub>x</sub> N <sub>y</sub>	Adsorbed gas species (N, molecular N <sub>2</sub> )	N <sub>2</sub> O
<b>1-shock treatment</b>				
3790 K	396.9	398.7	402.6	
3410 K	396.8	398.8	402.6	
3140 K	397.0	398.8	402.6	
1960 K	397.3	399.3	401.8	404.5
Pristine SiO <sub>2</sub>	397.1		401.8	
<b>2-shock treatment</b>				
3990 K	397.3		400.1, 402.5	404.7
3340 K	397.0	398.8	402.1	
3250 K	397.0		400.0, 402.5	
2250 K	397.0	398.6	402.4	
Pristine SiO <sub>2</sub>	397.1		401.8	

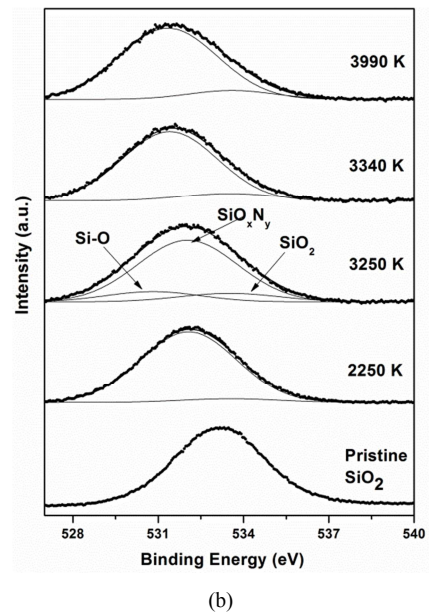
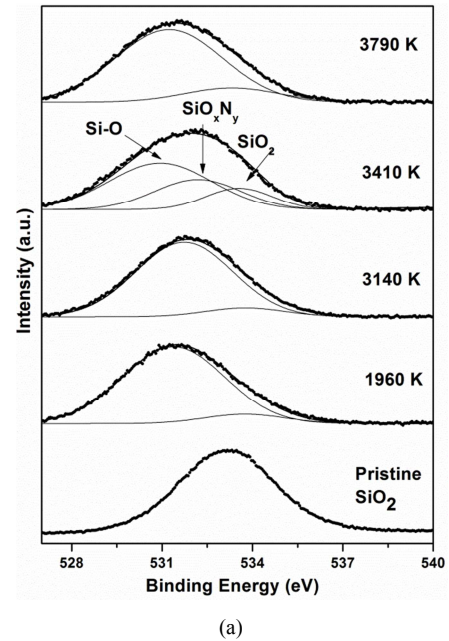
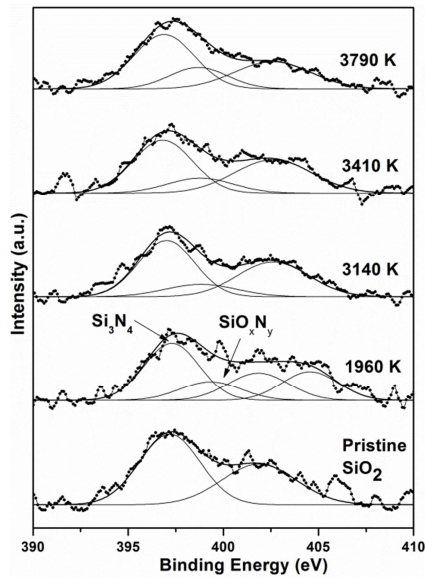
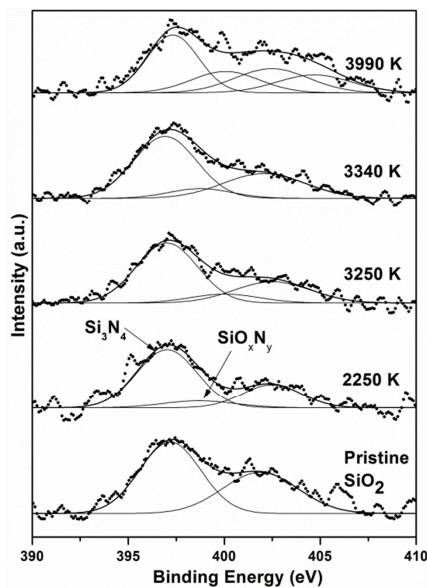


Figure 6. XPS of O1s core levels of SiO<sub>2</sub> powders before and after shock treatment at different temperatures: (a) 1-shock treatment and (b) 2-shock treatment.

Deconvoluted core level spectra of O1s before and after shock treatments are shown in Figure 6. O1s binding energy peak positions of different Si based compounds produced from SiO<sub>2</sub> samples with different shock-treated conditions are given in Table 3. The spectra of fresh SiO<sub>2</sub> powder indicate the peak corresponding to SiO<sub>2</sub> at 533.2 eV. After 1-shock treatment, the peaks due to SiO<sub>2</sub> are observed in the range of 533.3–533.7 eV which is similar to that reported in literature [23, 24]. The formation of oxynitride compounds, after 1-shock treatment, is evident from the peaks occurring at 531.2–532.2 eV. The similar trend is observed in the 2-shock-treated samples also and the respective peak positions are also listed in Table 3. In addition to this formation of SiO is also observed in few cases from the peaks at 530.8–530.9 eV.



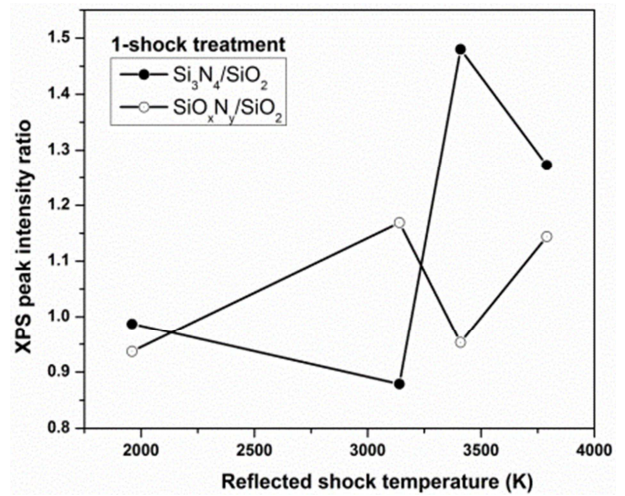
(a)



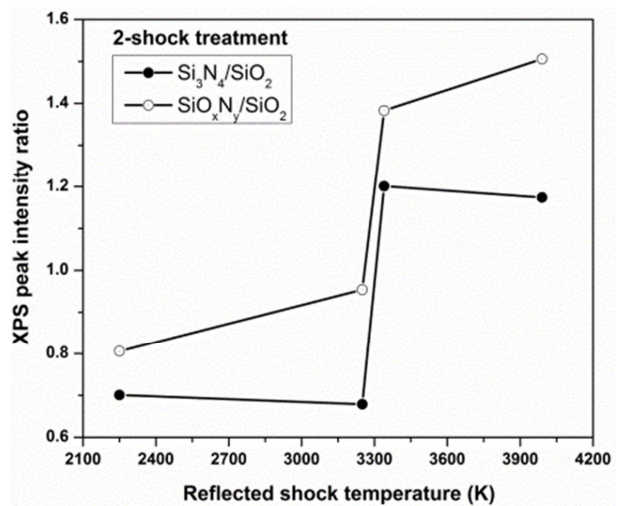
(b)

**Figure 7.** XPS of N1s core levels of SiO<sub>2</sub> powders before and after shock treatment at different temperatures: (a) 1-shock treatment and (b) 2-shock treatment.

The deconvoluted N1s core level spectra of shock-treated samples, shown in Figure 7, also reflects the presence of new compounds by showing peaks corresponding to silicon nitride at 396.8–397.3 eV for 1-shock and 2-shock-treated samples at different temperatures. The peaks due to silicon oxynitride in both 1-shock and 2-shock-treated samples are seen at 398.0–398.4 eV. The peaks are in reasonable agreement to those reported in the literature [25, 26]. There are few other peaks observed in some cases, occurring in the range 400.0–402.6 eV, which belong to the adsorbed N and molecular N<sub>2</sub> species [27]. Peaks attributed to N<sub>2</sub>O are also observed at 404.5–404.7 eV in few cases [28]. N1s binding energy peak positions of different Si based compounds produced from SiO<sub>2</sub> samples with different shock-treated conditions are presented in Table 4.



(a)



(b)

**Figure 8.** Intensity ratio of nitride and oxynitride peaks to oxide peaks of Si2p core level spectra: (a) 1-shock-treated samples and (b) 2-shock-treated samples.

The XPS results show the formation of the new nitride and oxynitride compounds confirming that non-catalytic surface reactions take place due to the interaction of SiO<sub>2</sub> fine

powders with shock-heated Ar+N<sub>2</sub> mixture gas. To understand the effect of shock temperature and the number of shock treatments on the SiO<sub>2</sub> powders, quantification of the formed silicon nitride (Si<sub>3</sub>N<sub>4</sub>) and silicon oxynitride (SiO<sub>x</sub>N<sub>y</sub>) is done. For the quantification, the intensity of the corresponding nitride or oxynitride peaks in the deconvoluted XPS is considered. Ratio of the peak intensities of the given nitride or oxynitride peak to that of the oxide peaks (SiO<sub>2</sub>) for each shock-treated sample is calculated and plotted in Figure 8. The presence of the nitride and oxynitride content is found to be more for high reflected shock temperatures.

In all the cases, the presence of both Si<sub>3</sub>N<sub>4</sub> and SiO<sub>x</sub>N<sub>y</sub> is observed. For 2-shock-treated samples, the content of the oxynitride is more in comparison with nitride compound. This increase in oxynitride after 2-shock treatment might be due to the formation of oxynitrides from the already present nitrides which are formed during the 1-shock treatment. The formation of such nitride and oxynitride compounds confirms that the SiO<sub>2</sub> fine powders have undergone a non-catalytic surface reaction upon interaction with shock heated nitrogen gas.

The XRD pattern indicates the formation of new nitrogen bonded SiO<sub>2</sub> compounds and unreacted compound after two shock treatment remains as amorphous SiO<sub>2</sub>. Upon shock interaction the irregular shaped SiO<sub>2</sub> particles become uniform micro and nano spheres as confirmed from the SEM and TEM micrographs. The interaction of shock waves with the powders results in the formation of new compounds as it is evident from the XPS studies.

#### 4. Fully Non-catalytic Surface Recombination Reaction

Shock-induced non-catalytic and catalytic reactions have been carried out using shock tube (MST1) in presence of shock heated nitrogen test gas. Heterogeneous non-catalytic surface recombination reaction occurs on the surface of SiO<sub>2</sub> fine powder in presence of high temperature N<sub>2</sub> gas at one and two shock treatment for about 2 ms test time. At this temperature, nitrogen can go to translational, vibrational excitation and dissociation states resulting in the three-body non-catalytic/catalytic surface recombination reaction as illustrated in Figure 9.

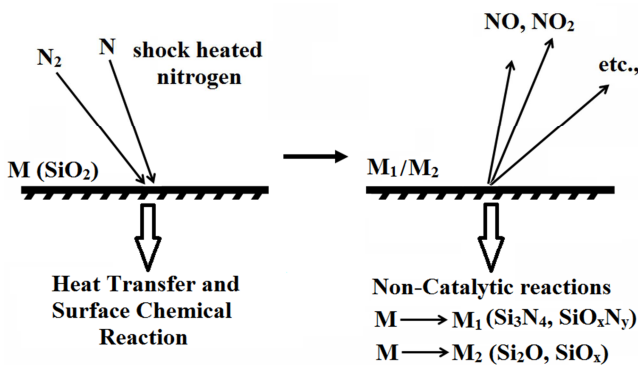
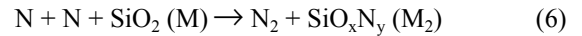
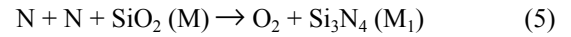


Figure 9. Schematic diagram of three body non-catalytic surface reactions.

Exposure to shock, mainly SiO<sub>2</sub> undergoes 3-body surface non-catalytic reaction by changing to different nitride compounds and also remains as SiO<sub>2</sub> due to catalytic surface reaction as illustrated in Figure 9 where M, M<sub>1</sub>/M<sub>2</sub> represent the surface of as-prepared and shock-treated SiO<sub>2</sub> fine powders, respectively. Reactions with high temperature N<sub>2</sub> molecule are shown below during which heat transfers from high temperature gas to materials (M) by forming new material M<sub>1</sub>/M<sub>2</sub>:



When a shock heated N<sub>2</sub> gas dissociates, the dissociated gas atoms recombine and transfer heat to the materials (third body M) by evolving O<sub>2</sub>, N<sub>2</sub>, N<sub>2</sub>O gas etc. as shown in the reactions below:



where M is SiO<sub>2</sub> and M<sub>1</sub> and M<sub>2</sub> are compounds of SiO<sub>2</sub> after shock treatment. During shock interaction, heat transfers from N<sub>2</sub> gas molecules to SiO<sub>2</sub> (M) by forming new compound is shown by analyzing its electronic structure and chemical composition.

In all these cases, heat transfers from gas molecules to third body (M), while the change in electronic structure and chemical composition of the third body are analyzed using different experimental techniques. From XRD and other characterization techniques, it has been concluded that change in crystal structure occurs due to heat transfer from shock heated test gases (N<sub>2</sub>). Surface heating is about 40% less for non-catalytic wall reaction [29]. SiO<sub>2</sub> fibers are used as TPS material in the form of silica tile in the re-entry space vehicles and capsules. SiO<sub>2</sub> undergoes both non-catalytic and catalytic surface reaction with different test gases, which reveals that it is a promising thermal protection material for aerospace and other high temperature applications. When a space vehicle enters into atmosphere at a speed of 2-8 km/s, gas around the shock layer experiences real gas effect. Gas species under such conditions interact with the ablated SiO<sub>2</sub> fine particles. Understanding the reaction of such ablated fine SiO<sub>2</sub> particles in the shock layer with high temperature nitrogen is of seminal importance in space applications during atmosphere re-entry.

#### 5. Conclusions

The interaction of SiO<sub>2</sub> fine powders with the shock-heated test gases has been demonstrated using shock tubes. The results clearly show the formation of new compounds such as silicon nitride and silicon oxynitride resulting from the surface reaction of SiO<sub>2</sub> with shock heated gases. XRD patterns of the shock-treated samples show that SiO<sub>2</sub> powders transform from crystalline to amorphous phase upon interaction with shock waves. The effect is more pronounced

in the higher shock temperatures and with the increasing number of shock treatments. The diffraction peaks corresponding to the new phases are also observed in the XRD patterns. SEM and HRTEM micrographs show that irregular shaped pristine SiO<sub>2</sub> forms uniform micro/nano spheres upon shock interaction. The presence of the newly formed nitride and oxynitrides are clearly observed from the XPS of the shock-treated samples. Nitride and oxynitride content is observed to be more for high temperature shock treatments. The formation of the new compounds is found to be due to the non-catalytic surface reactions of the SiO<sub>2</sub> powders which occur during the interaction of shock-heated Ar+N<sub>2</sub> test gas mixture.

## Funding

Financial supports for this project from ISRO-IISc STC, DRDO and DST, Government of India are gratefully acknowledged.

## Acknowledgements

The authors thank Professors K P J Reddy and G. Jagadeesh from the Department of Aerospace Engineering and Prof. E. Arunan, Inorganic and Physical Chemistry, Indian Institute of Science, Bengaluru for their support and fruitful discussions.

## References

- [1] P. A. Gnoffo, Planetary-entry gas dynamics, *Annu Rev Fluid Mech.* 31 (1999) 459–94.
- [2] C. D. Scott, Catalytic recombination of nitrogen and oxygen on high-temperature reusable surface insulation, 15<sup>th</sup> AIAA Thermophysics Conference, Snowmass, 14-16 July (1980).
- [3] T. Kurotaki, Construction of catalytic model on SiO<sub>2</sub>-based surface and application to real trajectory, 34<sup>th</sup> AIAA Thermophysics Conference, Denver, 19-22 June (2000).
- [4] E. H. Hirschel, *Basics of aerothermodynamics*, Springer, (2004).
- [5] M. Balat-Pichelin, J. M. Badie, R. Berjoan, P. Boubert, Recombination coefficient of atomic oxygen on ceramic materials under earth re-entry conditions by optical emission spectroscopy, *Chem. Phys.* 291 (2003) 181–194.
- [6] M. Barbato, S. Reggiani, C. Bruno, J. Muylaert, Model for heterogeneous catalysis on metal surfaces with applications to hypersonic flows, *J. Thermo. Heat Trans.* 14 (2000) 412–420.
- [7] K. Oguri, T. Sekigawa, J. Kochiyama, K. Miho, Catalytic measurement of oxidation-resistant CVD-SiC coating on C/C composite for space vehicle, *Mater. Trans.* 42 (2001) 856–861.
- [8] R. Morgan, Shock tubes and tunnels: Facilities, instrumentation and techniques, Chapter 4.3 Free piston-driven expansion tubes, In: *Handbook of Shock Waves*, vol. 1, (2001) 603–622.
- [9] P. Leyland, T. McIntyre, R. Morgan, P. Jacobs, F. Zander, U. Sheikh, T. Eichmann, E. Fahy, O. Joshi, G. Duffa, D. Potter, N. Banerji, J. Mora-Monteros, V. Marguet, Radiation-ablation coupling for capsule re-entry heating via simulation and expansion tube investigations, 5<sup>th</sup> European Conference for Aeronautics and Space Sciences (2013).
- [10] K. P. J. Reddy, M. S. Hedge, and V. Jayaram, Material processing and surface reaction studies in free piston driven shock tube, 26<sup>th</sup> International Symposium on Shock Waves, Gottingen, Germany (Plenary talk), 15-20 July (2007) Page 35–42.
- [11] V. Jayaram, Experimental investigations of surface interactions of shock heated gases on high temperature materials using high enthalpy shock tubes, Ph.D. Thesis. Bangalore (India): Indian Institute of Science, (2007).
- [12] V. Jayaram, R. Ranjith, H. K. T. Kumara, K. SubbaRao, K. P. J. Reddy, Investigation of non-catalytic reaction of shock heated nitrogen gas with powder SiO<sub>2</sub>, 30<sup>th</sup> International Symposium on Shock Waves, Tel Aviv, Israel, 19-24 July (2015).
- [13] I. Cozmuta, Molecular mechanisms of gas surface interactions in hypersonic flow, 39<sup>th</sup> AIAA Thermophysics Conf., Miami, FL, (2007).
- [14] K. Chen, Z. Huang, Y. Liu, M. Fang, J. Huang, Y. Xu, Synthesis of β-Si<sub>3</sub>N<sub>4</sub> powder from quartz via carbothermal reduction nitridation, *Powder Tech.* 235 (2013) 728–734.
- [15] A. N. Itakura, M. Shimoda, M. Kitajima, Surface stress relaxation in SiO<sub>2</sub> films by plasma nitridation and nitrogen distribution in the film, *Appl. Surf. Sci.* 216 (2003) 41–45.
- [16] W. Orellana, A. J. R. da Silva, A. Fazzio, Diffusion-reaction mechanisms of nitriding species in SiO<sub>2</sub>, *Phys. Rev. B* 70 (2004) 125206.
- [17] W. Guo, Y. Jia, K. Tian, Z. Xu, J. Jiao, R. Li, Y. Wu, L. Cao, H. Wang, UV-triggered self-healing of a single robust SiO<sub>2</sub> microcapsule based on cationic polymerization for potential application in aerospace coatings, *Appl. Mater. Interfaces* 8 (2016) 21046–21054. doi: 10.1021/acsami.6b06091
- [18] F. S. Miranda, F. R. Caliari, T. M. Campos, A. M. Essiptchouk, G. P. Filho, Deposition of graded SiO<sub>2</sub>/SiC coatings using high-velocity solution plasma spray, *Ceramics International* 43 (2017) 16416–16423. doi: 10.1016/j.ceramint.2017.09.018
- [19] A. G. Gaydon, I. R. Hurle, *The shock tube in high-temperature chemical physics*, 23–28, Reinhold Publishing Corporation, New York, (1963).
- [20] A. Thogersen, J. H. Selj, E. S. Marstein, Oxidation effects on graded porous silicon anti-reflection coatings, *J. Electrochem. Soc.* 159 (5) (2012) D276-D281.
- [21] D. C. Park, T. Yano, S. H. Kim, W. Y. Choi, J. H. Cho, Surface characterization of the milled-silicon nitride nano powders by XPS and TEM, *Key Engg. Mater.* 326-328 (2006) 409–412, doi: 10.4028/www.scientific.net/KEM.326-328.409.
- [22] A. L. Gerrard, J. J. Chen, J. F. Weaver, Oxidation of nitride Si (100) by gaseous atomic and molecular oxygen, *J. Phys. Chem. B*, 109 (2005) 8017–8028.
- [23] Y. Hijikata, H. Yaguchi, M. Yoshikawa, S. Yoshida, Composition analysis of SiO<sub>2</sub>/SiC interfaces by electron spectroscopic measurements using slope-shaped oxide films, *Applied Surface Science* 184 (2001) 161–166.

- [24] M. P. Albano, L. B. Garrido, Processing of concentrated aqueous silicon nitride slips by slip casting, *J. Am. Ceram. Soc.*, 81 (4) (1998) 837–844.
- [25] Y. Gu, L. Chen, Y. Qian, Low-temperature synthesis of nanocrystalline  $\alpha$ -Si<sub>3</sub>N<sub>4</sub> powders by the reaction of Mg<sub>2</sub>Si with NH<sub>4</sub>Cl, *J. Am. Ceram. Soc.* 87 (2004) 1810-1813.
- [26] Y. Xu, X. Zhu, H. D. Lee, C. Xu, S. M. Shubeita, A. C. Ahyi, Y. Sharma, J. R. Williams, W. Lu, S. Ceesay, B. R. Tuttle, A. Wan, S. T. Pantelides, T. Gustafsson, E. L. Garfunkel, L. C. Feldman, Atomic state and characterization of nitrogen at the SiC/SiO<sub>2</sub> interface, *J. Appl. Phys.* 115 (2014) 033502.
- [27] B. Viswanathan, K. R. Krishnamurthy, Nitrogen incorporation in TiO<sub>2</sub>: Does it make a visible light photo-active material? *Intl. J. Photoenergy* (2012) 269654. doi: 10.1155/2012/269654
- [28] S. H. Overbury, D. R. Mullins, D. R. Huntley, Lj. Kundakovic, Chemisorption and reaction of NO and N<sub>2</sub>O on oxidized and reduced ceria surfaces studied by soft X-ray photoemission spectroscopy and desorption spectroscopy, *J. Catalysis* 186 (1999) 296–309.
- [29] S. Kojiro, F. Kazuhisa, A. Takashi, Chemical nonequilibrium viscous shock-layer analysis over ablating surface of superorbital re-entry capsule, *The Institute of Space and Astronautical Science, Report SP No. 17, (2003) 24–41.*